EXPERIMENTAL INVESTIGATION OF EMULSION CHARACTERISTICS OF HIGH-WATERCUT OIL WELLS FOR DOWNHOLE SEPARATION PURPOSES

P.H. Janssen, W.M.G.T. van den Broek,
Delft University of Technology, Faculty of Applied Earth Sciences, Delft;
C.K. Harris,
Shell International Exploration and Production, Research and Technical Services, Rijswijk;
The Netherlands.

ABSTRACT

An experimental study has been executed to determine the morphology of oil-water mixtures which are produced into a high-watercut well. This information is an important factor in determining the feasibility of downhole oil-water separation
.
Core-flow and micro-flow experiments were performed to simulate the two-phase flow process in the near-wellbore region of a high-watercut well. In the core-flow experiments the morphology of oil-water mixtures leaving different types of porous media was observed and the droplet size distribution determined for different fluid properties and flow parameters. In the micro-flow experiments the flow regimes and breakup mechanisms of the oil phase were visualised and observed.

The results of the experiments show that the type of oil-water mixture emerging from the porous medium end face depends strongly on the wettability of the porous medium. When the porous medium is oil-wet the produced oil is mainly in the form of large drops which are formed at the porous end face. From water-wet porous media, at high flow rates, small oil droplets are produced whose sizes are typically of the order of the pore size and which are formed *inside* the porous medium. A correlation between the droplet size and relevant fluid, flow and porous medium parameters has been found, which allows the circumstances in which (downhole) separation can become problematic, to be assessed. Furthermore, the results of the experiments have shown that in water-wet porous media in the capillary number range investigated ($10^{-5}<Ca<10^{-3}$), a transition from capillary-dominated to dispersed flow takes place.

INTRODUCTION

Nowadays, huge amounts of water are produced together with the oil in mature oil fields. The water-cut of high-watercut oil wells can in some cases rise to almost 100 vol.% before the wells are abandoned, depending on the economics of the well. A new technology which could extend the economic lifetime of high-watercut oil wells is downhole separation. This technology comprises the (partial) separation of oil and water by a hydrocyclone mounted in the wellbore near the producing interval of the oil field. One factor determining the success, or otherwise, of this technology is the separation efficiency of the hydrocyclone,

which depends strongly on the morphology of the oil-water mixture flowing into it.

An experimental investigation has been carried out, aiming to establish the morphology of an oil/water mixture as present in the near-wellbore formation and produced into a well at high water-cut conditions. Two types of experiments were conducted, viz. core-flow experiments and micro-flow experiments. In the core-flow experiments the co-current flow of oil and water as occurring in the near-wellbore region was simulated by injecting both phases simultaneously into different types of porous media. The type of oil-water mixture leaving the porous medium was observed and characterised and the droplet-size distributions of any oil-in-water dispersions produced were measured by means of laser-diffraction. The flow, fluid and porous medium parameters were varied in the experiments and the water pressure was measured in the porous medium as function of distance from the inflow face
.
In the micro-flow experiments the flow regimes and breakup mechanisms taking place *in* the porous medium of a two-dimensional etched-glass model were observed during co-current flow of oil and water. The parameters varied were flow rate, oil-water ratio, oil viscosity, interfacial tension and wettability. The pressure drop over the model was also measured.

THEORY

The vertical inflow profile of a (high-)watercut well (see figure 1) is characterised by a top layer of oil, a bottom layer of water and an intermediate layer in which both phases are present. The presence of both phases in the intermediate layer is caused by static capillary forces and by a macroscopic instability at the oil-water interface upon flowing[1]. The interval over which both phases are present is given by the capillary transition height h_{cap} [m], which is the height of a column of the denser phase that can just be supported by capillary forces. It is given by

$$h_{cap} = \frac{2\, s\, \cos q}{r\, g\, \Delta r} \qquad (1)$$

where Dr [kg·m^{-3}] is the density difference between the oil and water phase, θ [-] and σ [kg·s^{-2}] respectively the contact-angle and interfacial tension of the oil-water interface and *r* [m] the pore radius which can be approximated by the squareroot of the permeability: √k. h_{cap} has about a value of 27 metres in a waterwet formation with a permeability of 1 Darcy.

In the pore space very close to a high-watercut well the capillary number *Ca* attains values typically between 10^{-3} and 10^{-5}, which can cause dispersion of the non-wetting phase. Several researchers[2,3] have investigated which two-phase flow regimes occur at the pore-scale in porous media as a function of capillary number. They found that in completely water-wet porous media the connected oil paths, which prevail at low capillary number, start to break up when the capillary number becomes larger than about 10^{-5}, provided the oil saturation is not too high. Upon increasing the capillary number from 10^{-5} to 10^{-3}, the flowing oil entities change from large ganglia, with a typical length of 10 pore-chambers, to so-called singlets, filling only one pore chamber. This result is consistent with the observation that during residual oil mobilisation from waterwet sandstone, the size of oil entities that can be mobilised at $Ca=10^{-3}$ is typical of the order of a pore body which explains the fact that at this capillary number the porous medium is nearly desaturated. In intermediate or oil-wet porous media the flow regimes occurring are very distinct from those observed in completely water-wet porous media. This is caused by the high value of the adhesion force between the oil and the oil-wet porous medium, compared to the water-wet case.

When the porous medium is completely water-wet a layer of water will always be present between the pore wall and the oleic phase. The phenomenon of breakup of oil in the porous medium under water-wet conditions is caused by two different mechanisms viz. snap-off and viscous break-up.

Snap-off is an interfacial instability which occurs when a non-wetting fluid entity passes a constriction, such as a pore-neck (see figure 2). After the head of the entity has protruded through the pore-neck the wetting liquid pressure at the head of the entity can become larger than in the neck region, resulting in flow of wetting fluid towards the neck region and decrease of the neck diameter. The difference in wetting fluid pressure is caused by the capillary pressure gradient present in the axial pore direction which is enforced by the decreasing non-wetting phase neck radius and explains the instability of the process. The snap-off process was in particular studied in the context of foam formation in porous media[4,5]. When dealing with snap-off of gas bubbles the gas pressure is equal and snap-off is initiated when the capillary pressure at the head becomes smaller than in the neck region.

When the process can be assumed (quasi-) static the moment of snap-off and the volume of the bubble being snapped off are completely determined by the geometry of the pore constriction. The radius of the bubble R_b [m] is in that case given by:

$$R_b \approx \frac{2\, R_n\, R_g}{(R_g - R_n)} \qquad (2)$$

provided that snap-off takes place. R_n [m] and R_g [m] are the radii of curvature in the neck of the bubble (see figure 2). Snap-off is favoured by large aspect ratio *A*, which is defined as the ratio of pore-body to pore-neck diameter: D_{body}/D_{neck}. In an orthorhombic glass-bead pack the aspect ratio is smaller than the minimum required aspect ratio A_{min} for static snap-off. Therefore snap-off in such a glass-bead pack can only take place theoretically at the end face where the aspect ratio is infinite. In real sandstone the aspect ratio can attain values up to ten, allowing snap-off inside the porous medium as well.

When the snap-off process becomes a dynamic process, the snap-off time and volume become a function of capillary number and fluid viscosity ratio as well and depend mainly on the speed of the drainage process of wetting fluid towards the neck region. This process is strongly dependent on the

shape of the pore cross section. The snap-off volume of gas bubbles was observed to increase with capillary number in square capillaries[4] in the capillary number range between 10^{-5} and 10^{-3}. When dynamic snap-off of oil entities is considered the squeezing of the oil in the neck-region is relevant as well. In experiments it was observed that no snap-off occurred at all when the viscosity ratio became too high, even when the aspect ratio was very high.

The second type of process which could be responsible for the breakup of oil ganglia in water-wet porous media is viscous breakup. This process has been only studied in simple linear flow fields such as simple shear flow and 2-D extensional flow[6,7]. The drop breakup process was analysed theoretically in these two types of flow and in 3-D extensional flow.

The results of the experimental investigations revealed that a drop with radius R [m] is broken up under steady conditions if a droplet-based capillary number Ca_{bu} is larger than a certain critical capillary number Ca_{crit} which is a function of the type of flow and the viscosity ratio only[7]:

$$\frac{t\ R}{s} > Ca_{crit}\left(\frac{m_d}{m_c},\ flow\,type\right) \qquad (3)$$

where τ [kg·m^{-}1·s^{-2}] is the deforming stress working on the drop in the flow field which is respectively equal to $m_c\dot{\varepsilon}$ and $m_c\dot{\gamma}$ in case of 2D-extensional and simple shear flow. The critical capillary number was determined experimentally for the above-mentioned flow types.

The maximum shear rate and strain rate in a porous medium can be approximated roughly by:

$$\dot{\gamma}_{\max} = \frac{4v}{\sqrt{8kf}} \qquad (4)$$

And:

$$\dot{\varepsilon}_{\max} \approx 1.8\frac{v}{f\sqrt{k}} \qquad (5)$$

where ϕ [-] is the porosity of the medium and v [m·s^{-1}] is the Darcy velocity.

If the drop capillary number is more than five times greater than the critical capillary number the deformation becomes unsteady and the drop will deform into a thread[8]. During extension of the thread or during relaxation after stress release the thread can disintegrate into many small droplets caused by pressure gradients in the thread which are induced by interfacial waves.
The breakup of drops in chaotically changing flows such as flow through porous media was simulated numerically by applying high-order linear deformation theory on drops flowing through dense packs of beads. The results showed that breakup of drops in this type of flow even can occur for subcritical values of the drop capillary number.

The effect of porous medium wettability on droplet formation can be demonstrated by considering the theoretical work of Koretskii[9] who analysed the thermodynamics of the detachment of an oil drop from a solid substrate surrounded by an aqueous solution, as a function of contact angle and interfacial tension (see figure 3). The minimum amount of mechanical work A_M [kg·s^{-2}] that has to be employed to remove a droplet from a substrate is the sum of work A_a to overcome the adhesion force and the work A_D to change the surface energy of the system:

$$\begin{aligned} A_M &= A_a + A_D \\ &= \frac{s\,(1-\cos q)}{S_1^d} + \frac{s\,(\Sigma S_d - S_1 - S_2)}{S_1^d} \end{aligned} \qquad (6)$$

where S_1 [m^2] and S_2 [m^2] are respectively the surface area between drop and aqueous solution and between the drop and substrate before detachment. SS_D [m^2] is the sum of surface area of the newly formed droplets after detachment and S_1^d [m^2] is the minimum surface area of the oil in solution.
The analysis shows that the work necessary for to remove oil from an oil-wet surface ($\theta\rightarrow180^o$) requests a minimum amount of work, which is 5 to 6 orders of magnitude larger than in the water-wet case ($\theta\rightarrow0^o$). Furthermore it is demonstrated that removal of oil from oil-wet surfaces only can be done by dispersion of the oil into many small droplets.

Core-flow experiments

To examine the characteristics of oil-water mixtures flowing into an high-watercut oil well core-flow experiments were performed, whereby the simultaneous flow of oil and water as occurring in the near-wellbore region of a high water-cut well was imitated. The main objective was to observe and characterise the oil-water mixtures leaving different types of porous media under different production conditions and to measure the size-distributions of the emulsion droplets produced. The parameters varied in the core flow experiments were:

1. Production parameters, i.e. production flow rate Q and oil concentration.
2. Porous medium properties, i.e. permeability k, porosity ϕ and wettability.
3. Fluid properties, i.e. oil viscosity μ_o and interfacial tension σ.

The experimental set-up. In Figure 4 a schematic overview of the experimental set-up used for the core-flow experiments is depicted. Oil and water are both pumped via a special inlet piece into a cylindrical core. The core is mounted vertically in a core holder and the effluent can be observed via a viewing glass connected to the upper side of the core. The water is de-aerated and filtered before being pumped through the core. The oil reservoir is put under pressure to prevent vapour bubbles being formed at higher oil flow rates. The effluent from the core passes through the measurement cell of a laser diffraction-based particle size analyser and can eventually be diluted by tap water. The effluent can also bypass the measurement cell to prevent it from becoming polluted. Finally the oil-water mixture is separated by an oil-water separator. During a flow experiment the pressure at positions along the core can be measured with a pressure sensor, measuring the pressure at the inlet of the core, and at nine pressure difference transducers.

Porous medium samples. Three types of porous media were used in the experiments, viz.:

1. Six different kinds of outcrop sandstone, all being water-wet. The permeability k, porosity ϕ and tortuosity Υ of the different cores were measured and the values are depicted in Table 1. Also the capillary pressure curves for mercury intrusion porosimetry were measured and were converted to a pore-neck-size distribution.
2. The sandstone samples could eventually be made oil-wet by a chemical silylation process whereby the H-atoms of the surface hydroxyl groups of the silica surface are bounded by covalently bound organosilyl groups.
3. Four cores composed of glass beads with different diameter, glued together by epoxy resin. The resin, which renders the core oil-wet, is located between the contact points of the glass beads and forms a thin layer on the surface of the beads. The properties of the glued glass-bead cores are depicted in Table 2.

All cores had a diameter of 2.5 cm. The length of the sandstone and glued glass bead cores was respectively 5 and 10 cm. The cores were mounted in a steel cylinder using epoxy resin.

Fluids. The fluids used in the experiments were tap water, de-aerated and filtered before use, and Shell Vitrea mineral oil with three different viscosities, viz. Shell Vitrea 9, 46 and 68. The oil is composed of different paraffinic oils without any additives. The properties of the oils used are given in Table 3 and are measured at a temperature of 20 ^{o}C. The interfacial tension σ is measured in relation to tap water.

The interfacial tension between the fluids could be lowered by adding Iso Propyl Alcohol (IPA) to a mixture of oil and water. After waiting for equilibrium between the different components for some hours the phases were separated again. The aqueous phase was proven to wet the sandstone samples completely in combination with the oleic phase. The 3 fluid systems used in the experiments and their properties are given in Table 4.

Experimental Procedures and Program. Different types of experiments were performed to mimic the simultaneous flow of oil and water in the near-wellbore region of a high-watercut oil well and to determine which flow regimes and droplet formation mechanisms are occurring under these conditions as function of the different parameters, viz.:

1. An oil-water mixture with 1 vol.% oil was injected into the 6 types of water-wet sandstone and the 4 different glass-bead cores. The droplet-size distributions and pressure drops over the cores were measured, after steady state was achieved, for flow rates Q varying between 50 and 2000 ml/min. These flow rates correspond to a capillary number range between 5.7×10^{-5} and 1.1×10^{-3}. This was done for the three oil viscosities.
2. An oil-water mixture with 1 vol.% oil was injected into a (water-wet) Bentheim sandstone core. Again the droplet-size distribution and the pressure drops were measured for varying flow rate. This was done

for Vitrea 9 and 68 oil. Later on the core was made oil-wet by the silylation process and the experiments were repeated.
3. The impact of interfacial tension between the wetting and non-wetting phase on two-phase morphology was investigated by using the 3 fluid systems, given in table 4. The droplet-size distributions of the non-wetting phase were determined for varying flow rate when 99 vol.% of the wetting phase and 1 vol.% of the non-wetting phase were injected in a water-wet Bentheim sandstone core with a length of 40 cm ($k=1.85\cdot10^{-12}$ m^2, $\phi=0.23$).
4. The impact of oil content on oil droplet-size distribution was investigated by simultaneous injection of Vitrea 9 oil and water in a (water-wet) Berea sandstone core ($k=1.2\cdot10^{-12}$ m^2, $\phi=0.226$). The total flow rate was kept constant at 110 ml/min while the oil percentage was varied between 1.1 and 14.8%. The same type of experiment was done with an oil-wet-made Bentheim sandstone core whereby the oil content was varied between 1.0 and 11.8% at a total flow rate of 160 ml/min.
5. The pressure profile along a Bentheim core during simultaneous steady flow of oil and water was studied by injecting subsequently 0.26, 0.52, 1.04, 2.08 and 4.16% of oil at a constant flow rate of 108 ml/min. The core had a length of 40 cm. Next the oil percentage was decreased again using the same sequence of values in reverse. This was done for Vitrea 9 and 68 oil. The same experiment was repeated again but with an initial oil percentage of 0.52 vol.%. Also the oil droplet-size distributions were measured.

Another test was done by injecting 1 vol.% of Vitrea 9 oil in a water-wet Clashach sample at a constant flow rate of 572 ml/min. Subsequently, the oil percentage was decreased several times till the oil percentage became 0.17 vol.%. The pressure along the core and the corresponding droplet-size distributions were measured.
During all these experiments the effluent face of the cores and the oil-water mixtures leaving the cores were observed.

Micro-flow experiments

Micro-model. The micro-flow experiments were performed with a two-dimensional micro-flow model consisting of two symmetrically etched glass plates (figure 5). The porous area has a length of 6.0 cm and a width of 3.0 cm and consists of 3545 grains with a uniform diameter-size distribution between 190 and 440 μm. The surface porosity of the grain-filled area is 50.7%. In between these grains the glass is etched with a maximum depth of 35 μm (the pore height is thus 70 μm).
On the right-hand side of the model as depicted in figure 5, two inlet ports are present, which are split up into 4 supply channels. The right port was used as inlet for both phases and the left port was connected to a pressure sensor. At the left-hand end of the grain-filled area the model has been machined to a greater depth to mimic the end face of a porous medium, allowing droplet growth to occur. The depth of this drainage area is 360 μm. The permeability of the model is 32.1 Darcy. Both fluid phases leave the model through the left port.

Fluid systems. In the micro-flow experiments four different fluid systems were used for which the interfacial tension and viscosity ratio of the phases were varied. The basic fluids used were filtered de-mineralised water as the wetting phase and n-decane, Vitrea 9 or Vitrea 46 oil as the non-wetting phase. IPA was added to the liquids to lower the interfacial tension of the fluid system. Consequently the viscosity of the original basic wetting and non-wetting fluids was altered. The interfacial tension was measured with the Du Nouy-ring method at 20°C. The properties of the 4 fluid systems are depicted in Table 5.

Procedures and experiments. Before each experiment the glass plates were immersed in boiling 90% hydrogen peroxide for 10 minutes to obtain complete water-wet conditions. Subsequently, the plates were rinsed with de-mineralised water.
The experiments were performed by injecting wetting and non-wetting fluids of the fluid systems described into the water-wet model. The percentage of non-wetting fluid phase applied in the experiments was respectively 5 and 10 vol.% for the four fluid systems. In case of fluid systems I and III also non-wetting fluid phase percentages of 50 and 90 vol.% were applied.
The flow phenomena and droplet formation mechanisms were observed and the pressure drop at the inlet port was measured in case of high-watercut conditions (i.e. 5 and 10 vol.% non-wetting phase). After the experiments were performed under water-wet conditions, the glass plates were rendered oil-wet by chemical silylation, applying the same procedure as in the case of the sandstone cores. An experiment, using fluid system I and 10 vol.% decane, which is the wetting fluid phase, was performed with the oil-wet model.

Results of core-flow experiments

General Results. Qualitatively, two different oil-water morphologies could be observed leaving the porous media during simultaneous flow of oil and water viz.:

- a cloud of tiny oil-in-water droplets or an oil-in-water dispersion from which the size distribution could be measured with the particle size analyser
- large oil drops with diameters ranging from about 0.5 mm to several millimetres, from now on called *mm-drops*, which were generated by a drop growth mechanism directly at the end face of the porous medium.

The droplets dispersed in the cloud could be divided in two types (see figure 6):

Droplets with sizes of the order of the pores: 10-100 μm, from now on called *mm-droplets*.

❷ Super-pore sized droplets of about 100-500 μm.

The super-pore sized droplets were generated mainly at low capillary number (or pressure gradient) and a transition to the formation of μm-droplets occurred when the capillary number was increased (or pressure gradient). It appeared that μm-droplets were generated if the pressure gradient exceeded a critical value of about 100 bar/m.

This study was mainly focused on the occurrence and size distribution of the μm-droplets since they are most critical with respect to production processing, i.e. phase separation.

The impact of the different parameters, varied in the experiments, on both the μm-droplet size and the oil volume fraction of the μm-droplets, will now be summarised.

Wettability. The wettability of the porous medium appeared to be a very important parameter: water-wet sandstone cores produced mainly a cloud of tiny oil-in-water droplets (figure 6) whereas the oil left the oil-wet sandstone cores and glued glass bead cores in the form of large mm-drops. Only at very high flow rates were tiny oil-droplets also produced from the oil-wet cores.

Flow rate. The modal diameter of the μm-droplet distribution is plotted as function of flow rate for the different sandstone samples when 1 vol.% oil was injected (figure 7). It can be seen that the diameters decrease with increasing flow rate and that the droplet diameters are larger for cores with higher permeability or pore-neck diameter. When the modal droplet sizes are plotted as function of pressure gradient (see figure 8) all curves appear to overlap each other very well, which is a quite striking result. The unique curve can be described by the following correlation for pressure gradients larger than 100 bar/m:

$$D_{mm-droplet} \approx C\left(\frac{1}{\nabla p}\right)^{n} \qquad (7)$$

where *C* is a constant and the exponent *n* is close to a half: ***n*** » **0.5**. The mode diameters of μm-droplets which leave the different glued glass bead cores also seem to show a unique dependency of pressure gradient (figure 9). The pressure gradient is estimated using the one-phase pressure gradient in this case since the pressures were too low for measurement with the pressure transducers.

Interfacial Tension. In figure 10 the modal μm-droplet diameter is plotted as function of pressure gradient for the three different fluid systems when 1 vol.% of oleic phase is injected in the water-wet Bentheim sandstone. The exact values of the exponent *n* are depicted in the graph and seem to be close to *n*=0.5 similar to the results without lowering of the interfacial tension. Therefore, the dependency of μm-droplet diameter on pressure gradient is still given by eq. 7, but the modal droplet diameters are smaller for decreasing interfacial tension.

Oil viscosity. The modal μm-droplet diameter increases slightly for increasing oil viscosity in the case of water-wet sandstone samples. The relationship between droplet diameter and pressure gradient is still given by eq. 7, with *n* again close to 0.5.

In case of glued glass-bead cores, the μm-droplet diameter is larger for smaller oil viscosity at similar pressure gradient (or flow rate), a surprising result.

Oil fraction. The μm-droplet diameter distribution does not change significantly upon variation of the oil concentration between 1 vol.% and 14.8 vol.% in a waterwet sandstone core. For oil concentrations above about 5 vol.%, many mm-drops were also formed at the end face of the core. The volume ratio of oil present in the form of μm-droplets and mm-drops could not be determined exactly.

When the oil fraction was varied in an oil-wet sandstone core between 1.0 and 11.8 vol.%, the majority of the oil left the core as large mm-drops. The size distribution of the μm-droplets did not change significantly.

Pressure measurements. The pressure gradient in the different water-wet sandstone cores was measured as function of flow rate when 1 vol.% of oil was injected. A pseudo-relative permeability to water k_{rw} can be defined as ratio of the one-phase pressure gradient to the two-phase pressure gradient:

$$k_{rw} = \frac{\nabla P_1}{\nabla P_2} \qquad (8)$$

This pseudo-relative permeability value represents the relative resistance that the water phase experiences due to the presence of the oil phase. The relative permeability values are plotted in figures 11 and 12, for Vitrea 9 and 16 oils, respectively, as a function of pressure gradient when 1 vol.% oil is injected for all water-wet sandstone cores. The k_{rw}-curves for the high-permeable cores seem to show a strong increase at small pressure gradient and an approximately constant value at high pressure gradient. The k_{rw}-curves for the low–permeabele cores only show a constant value at higher pressure gradient. In case of Vitrea 9 oil the increase of the relative permeability value seems to occur faster, at pressure gradients smaller than 150 bar/m, compared to the case when Vitrea 46 oil is used. In that case the increase occurs at pressure gradients smaller than 200 bar/m.
Furthermore it can be seen that the k_{rw}-values for Vitrea 9 oil are slightly smaller.
From the pressure-profile measurements along the water-wet Bentheim sandstone core for varying oil concentrations *at relatively low capillary number* ($Ca \approx 1.2 \times 10^{-4}$) it could be observed that the pressure gradient along the core is constant and increases with injected oil concentration. Furthermore, it could be observed that no significant difference in pressure gradient exists during drainage or imbibition at the same oil concentration.
From the pressure-drop measurements along the water-wet Clashach sandstone core for different oil concentrations *at relatively high capillary number* ($Ca \approx 6.2 \times 10^{-4}$) it could be observed that the pressure drop did not change upon changing the oil concentrations and that droplet-size distributions of droplets leaving the core for different oil concentrations were *completely* identical.
The implications of these observations will be discussed later on in this paper.

Results of micro-flow experiments

Observations in water-wet model. Observations in the water-wet micro-model showed that for high and moderate water fractions (5, 10 and 50 vol.% non-wetting fluid phase) three capillary number ranges could be distinguished in which different flow mechanisms and dispersion phenomena occurred, viz.:

$Ca < 10^{-4}$: Decane flowed as connected pathways or as large ganglia through the model and at the end face where the grain-filled area ceased, droplets were formed very quickly by a snap-off process. At relatively high flow rate (within this Ca-number range) the droplet formation frequency was very high, in the order of 10 droplets per second, and the droplet size seemed to be weakly dependent on flow rate. At very low flow rates the formation frequency decreased and the droplet sizes increased slightly. The size of decane droplets ejected at the end face from a single pore was very homogeneous but varied significantly for different pores. No snap off was observed in the pore space of the model. This flow regime was defined *as capillary-dominated flow*.

❷ $Ca > 5 \times 10^{-4}$: The flow process was characterised by very rapid movement of decane droplets through the porous model, following the flow lines of the water. The droplets had sizes significantly smaller than the average pore width, i.e. grain-to-grain distance, but were in the order of the pore height. The velocity of the droplets was too rapid for good visualisation. Such droplets could only be observed within the porous medium on trapping behind a grain. The droplets which were formed in the porous model left the grain-filled area without undergoing any interactions that changed their size. The droplet diameter seemed to decrease with capillary number. No residual decane saturation was present in the porous area. This flow regime is defined as *dispersed flow*.

$10^{-4} < Ca < 5 \times 10^{-4}$: In this capillary number range a combination of the phenomena which occurred in the capillary-dominated and dispersed flow regime was observed, depending on the decane percentage and on the momentaneous local decane saturation. The cause of the fluctuation in decane saturation was that the fluid phases could not be injected completely homogeneously. When the instantaneous decane saturation was high, the droplets formed in the model coalesced again instantaneously and rivulets of decane broke up at the end face. When the momentaneous decane saturation was low the decane was dispersed in the porous medium and could leave the model without undergoing coalescence.

Impact of non-wetting phase viscosity
Experiments with Vitrea 9 and 46 oil showed similar results as those described for the experiments with decane, but the transition between the described flow regimes seemed to occur at a slightly higher capillary number for a higher oil viscosity.

Observations in 'oil-wet' model
The micro model appeared to be intermediate to slightly oil-wet after silylation. In the capillary number range investigated, $10^{-4}<Ca<8\times10^{-4}$, a layer of decane was formed at the end face through which the water penetrated by forming large water drops from certain pores, both for high and low water fraction. At low capillary numbers, both phases were forming static 'rivulets', whereas at high capillary numbers the flow was characterised by moving oil-water interfaces. No snap-off process or formation of small droplets, i.e. droplets of the order of the pore size, were observed in this capillary number range in the silylated model. Oil and water left the outlet of the model as continuous phases.

Pressure measurements
The pressure drop over the water-wet micro model was measured for one-phase and two-phase flow. The one-phase pressure drop as a function of flow rate showed a straight line, implying that Darcy's law was still valid at the flow rates applied. When two phases were injected, they were not distributed completely homogeneously over the pore space, especially at low flow rates. In the central part of the model the oil saturation was somewhat higher compared to the region near the 'wall'. Nevertheless, the pressure drop data was recorded several times and averaged to investigate possible relationships between these data and the flow mechanisms observed. A pseudo relative permeability value, k_{rw} was calculated, in the same way as for the core-flow experiments (see eq. 8). Figure 13 shows the k_{rw}-values plotted as a function of capillary number for the different fluid systems used (see Table 5) and for the cases of 5 and 10 vol.% non-wetting fluid phase injection. The capillary number is calculated using the Darcy flow velocity as the characteristic velocity. The relative permeability values increase with increasing capillary number and seem to become constant at high capillary number. The k_{rw}(Ca) curves are situated at lower values of k_{rw} when the viscosity ratio or the interfacial tension are high. When the viscosity ratio is low (fluid systems I and III), the curves coincided completely for non-wetting fluid phase percentages of 5 and 10 vol.% in contrast to the curves of fluid systems with high viscosity ratio. The pseudo-relative permeability values for fluid system III become slightly larger than 1 when the capillary number becomes sufficiently high. This is caused by the non-wetting fluid phase viscosity being smaller than the wetting fluid phase viscosity.

Discussion

The results of the core-flow and micro-flow experiments reveal that the type of oil-water mixture, being produced by a porous medium under typical near-wellbore flow conditions, strongly depends on the wettability of the porous medium. Oil-wet sandstone cores and glued glass-bead packs produce mainly mm-drops whereas water-wet sandstone cores produce mainly small emulsion droplets. These observations can be explained by the analysis of Koretskii[9] (see theory). In case of water-wet porous media a water film is present between the oil and the pore walls and the oil phase can be broken up relatively easy. In case of oil-wet porous media relatively much mechanical work needs to be exerted by the water flow to remove oil from the pore walls as shown by Koretskii. At low flow rate insufficient mechanical work is exerted on the oil located on the pore walls by the water flow to disperse it. Nevertheless, at very high flow rates, in particular from low-permeable cores, also some small droplets are produced from oil-wet porous media. In that case sufficient mechanical energy is exerted on the oil phase by the water flow to detach and emulsify (a part of) the oil in the pore space. When the oil is not emulsified in the porous medium, it will be flowing in the form of a film on the pore walls, driven by the water flow. Finally, the oil will accumulate at the end face, forming large drops, which will detach by hydrodynamic forces, especially the Stokes drag force.
The super-pore sized droplets which are produced from water-wet sandstone cores at low capillary number seem to correspond to droplets that were formed at the end face from the micro-model during capillary-dominated flow by snap-off. The sizes of the super-pore sized droplets, which are much larger than the pore neck diameter of the porous medium, are formed at the end face, possibly by snap-off.
The μm-droplets which are produced from water-wet sandstone cores at high capillary number seem to correspond to the droplets observed in the micro-model during dispersed flow. This implies that μm-droplets are formed *inside* the porous medium. This hypothesis is enforced by the fact that the μm-droplets have sizes of the order of the pore size.

The existence of a transition in flow regime from capillary-dominated to dispersed flow as observed in the micro-flow experiments seems to be confirmed by the results of the pressure measurements which

were done in a water-wet sandstone at 'low' and 'high' capillary number. At low capillary number, increasing the oil percentage caused an immediate increase of the pressure gradient in the core whereas at high capillary number variation of the oil percentage almost did not alter the pressure drop. The only plausible explanation for this phenomenon is that in case of dispersed flow, the increase of oil percentage causes no significant increase of the flow resistance to the water phase, because of the lubrication effect.

Another indication that a transition of flow regime occurs, which corresponds to the different types of droplets observed (i.e. super-pore sized and μm-droplets) is the strong increase of pseudo-relative permeability $k_{r,w}$ upon increasing the flow rate or pressure gradient (see figure 11 and 12).
A dimensional analysis was executed on the *m*m-droplet diameters measured from all experiments whereby 1 vol.% non-wetting phase was injected in water-wet cores, to obtain a satisfying scaling. It was assumed that the droplet diameter $D_{mm-droplet}$ is a function of pressure gradient $\tilde{N}p$, interfacial tension s, permeability *k* and fluid viscosities m_c and m_d. The results show that a scaled droplet diameter is a function of capillary number and viscosity ratio:

$$\frac{D_{mm-droplet}}{\sqrt{k}} \approx c\, Ca^{-1/2} \left(\frac{m_d}{m_c} \right)^{1/6} \qquad (9)$$

where *c* is a constant with value 446500 and *Ca* is the capillary number defined as $k\tilde{N}p/s$. The constant *c* and the exponents on the right-hand side of the correlation were determined by linear regression. The quality of the correlation is given in figure 14, where the measured droplet diameter D_{meas} is plotted as function of the correlated droplet diameter D_{corr} given by eq. 9. All data points lie within a 20%-interval from the ideal curve with slope 1. Furthermore, this correlation is consistent with eq. 7.
This correlation predicts that for example in case of production from a high-watercut well in a formation with a permeability of 100 mDarcy, the resulting dispersion becomes difficult to separate ($D_{mm-droplet} < 20\,mm$) if the capillary number in the near-wellbore region becomes larger than 6×10^{-4}, which is a value that might well be encountered in practice.
The relationship between the measured droplet sizes and the physical parameters can not be ascribed qualitatively to the mechanisms of snap-off or viscous breakup as described in this paper. The snap-off volume of a bubble in a square capillary (which is the geometry that resembles most to a realistic pore geometry) appeared to increase with capillary number[4] which does not correspond to the trend observed in our experiments.

The deforming stresses τ in the pore space, which can be estimated for our experiments with eq. 4 and 5, are one order of magnitude too small to obtain the droplets according to the theory of steady viscous drop breakup. Nevertheless, numerical simulations of droplet break-up in chaotic flow fields[10] have demonstrated that viscous drop breakup can occur at capillary numbers which are significantly smaller than the critical value under steady conditions. This indicates that the unsteady chaotic nature of flow through porous media is essential with respect to non-wetting phase break-up. Therefore, it has to be concluded that although the theories available in literature of snap-off and viscous breakup can not explain our results, these mechanisms still could be responsible for the breakup of oil in the pore space. Probably, the models are too simple and lack facets, which are essential for the processes.

CONCLUSIONS

Laboratory experiments have shown that during two-phase flow under near-wellbore conditions in water-wet porous media, oil-in-water emulsions can be formed which can cause problems with respect to (downhole) separation. The oil droplets are formed by dispersion in the pores of the near-wellbore region.
Emulsion droplet sizes appear to be a function of pressure gradient and interfacial tension.
Furthermore, the experiments have shown that emulsification of oil occurs at much higher capillary number if the porous medium is oil-wet. This information could be used to enhance the conditions for (downhole) separation.

TECHNICAL CONTRIBUTIONS

With the insight obtained from the results of the experimental investigation reported here the type of oil-water mixture entering a high-watercut well can be predicted. In the case of a water-wet rock formation the oil produced into such a well mainly comprises small μm-droplets which could cause problems with respect to (downhole) oil-water separation. This paper presents a correlation (eq. 9) with which the droplet diameter of these small droplets can be estimated as function of flow, fluid and rock properties.

Furthermore, guidelines for enhancing the conditions for oil-water separation are proposed in this paper.

REFERENCES

1. Raghavan, R., and Marsden, S.S., *A theoretical study of the instability in the parallel flow of immiscible liquids in a porous medium*, Quart. J. Mech. and Appl. Math. **26** (2), 1973.
2. Elsik, C.M. and Miller, C.A., *Videomicroscopy of Two-Phase Steady Cocurrent Flow in a Porous Medium*, Proc. 61st Annu. ACS Coll. & Surf. Sci. Symp. (ACS symp. ser. no. 373), 1988, p. 258-281.
3. Avraam, D.G. and Payatakes, A.C., *Flow regimes and relative permeabilities during steady-state two-phase flow in porous media*, J. Fluid Mech. **293**, p. 207-236 (1995).
4. Ransohoff, T.C., Gauglitz, P.A. and Radke, C.J., *Snap-off of gas bubbles in smoothly constricted noncircular capillaries*, AIChE Journal, 33 (5), 753-765, May 1987.
5. Gauglitz, P.A. and Radke, C.J., *The dynamics of liquid film breakup in constricted cylindrical capillaries*, J. Coll. Int. Sc., 134 (1), Jan. 1990.
6. Taylor, G.I., *The formation of emulsions in definable fields of flow*, Proc. R. Soc. A, 146, 501, 1934.
7. Grace, H. P., *Dispersion phenomena in high viscosity immiscible fluid systems and application of static mixers as dispersion devices in such systems*, Chem. Eng. Commun., 14, 225, 1981.
8. Janssen, J., *Dynamics of liquid-liquid mixing*, PhD-thesis, Eindhoven, The Netherlands, 1993.
9. Koretskii, A.F., Kolosanova, V.A., *Mechanical work of cleaning and washing effect of surfactant solutions*, translated from Kolloidnyi Zhurnal, 45 (1), 74-80, Jan. 1983.
10. Mosler, A.B., *Microstructure conformation change in stochastic flow fields: flow through fixed beds*, PhD-thesis, Stanford Univ., August 1997.

LEGEND OF ILLUSTRATIONS

Table 1 to 5: see tables
Fig.1 to Fig.6: see figures
Figure 7: Modal droplet diameter (i.e. mode of droplet size distribution) versus flow rate for different sandstone types and Vitrea 9 oil
Figure 8: Modal droplet diameter versus pressure gradient for different sandstone types and Vitrea 9 oil
Figure 9: Modal droplet diameter versus estimated pressure gradient for different glued glass-bead sizes and oil viscosities
Figure 10: Modal droplet diameter versus pressure gradient for different values of the interfacial tension
Figure 11: Dependence of pseudo-relative permeability on pressure gradient for a non-wetting phase injection rate of 1% in water-wet sandstones with Vitrea 9 oil
Figure 12: Dependence of pseudo-relative permeability on pressure gradient for a non-wetting phase injection rate of 1% in water-wet sandstones with Vitrea 46 oil
Figure 13: Pseudo-relative permeability versus capillary number in the micro-flow experiments for the different fluid systems, given in table 5
Figure 14: Data points showing the measured droplet diameter as a function of the correlated droplet diameter, given by eq.9; the line with unit slope is the ideal curve

Sandstone	k [mDarcy]	ϕ [%]	Υ [-]
Fontainebleau	3780	22.2	2.59
Bentheim	2500	22.6	2.52
Berea-high	2120	22.8	2.96
Berea-medium	790	23.6	2.61
Clashach	520	16.0	3.71
Kirchheim	950	19.4	2.81

Table 1: Properties of sandstone samples (water-wet)

Mean Glass Bead Size [μm]	ϕ [%]	k [Darcy]	k_{CK}^{*} [Darcy]
98.0	37.56	7.1	9.1
196.0	38.27	33.9	39.3
327.5	38.50	91.7	112.4
462.5	39.36	158	246.3

Table 2: Properties of glued glass-bead cores (oil-wet)
(* theoretical permeability according to Carman-Kozeny relationship)

Oil Type	ρ [kg/m^3]	μ [mPa.s]	σ [mN/m]
Shell Vitrea 9	868	15.2	29.9
Shell Vitrea 46	877	123	36.0
Shell Vitrea 68	882	198	19.9

Table 3: Properties of used mineral oils

	Volume fractions %			μ_w	μ_{nw}	ρ_w	ρ_{nw}	σ
	Tap-water	Vitrea 9 oil	IPA	[mPa.s]	[mPa.s]	[kg/m^3]	[kg/m^3]	[mN/m]
System 1	-	-	0.0	1.0	15.2	1000	868	31.2
System 2	85.6	7.8	6.6	1.32	15.6	989	874	18.6
System 3	71.5	6.5	22.0	2.44	15.9	971	877	9.9

Table 4: Properties of different fluid systems used in core-flow experiments

Fluid System	Components	Volume Fraction [%]	μ_d [mPa.s]	μ_c [mPa.s]	μ_d/μ	IFT [mN/m]
I	Water	-	1.0	1.0	1.0	36.3
	n-decane	-				
II	Water	-	15.2	1.0	15.2	31.2
	Vitrea 9	-				
III	Water	57	1.18	2.31	0.51	8.0
	IPA	24				
	n-decane	19				
IV	Water	62	14.2	1.7	8.4	10.0
	IPA	19				
	Vitrea 9	19				

Table 5: Properties of different fluid systems used in core-flow experiments

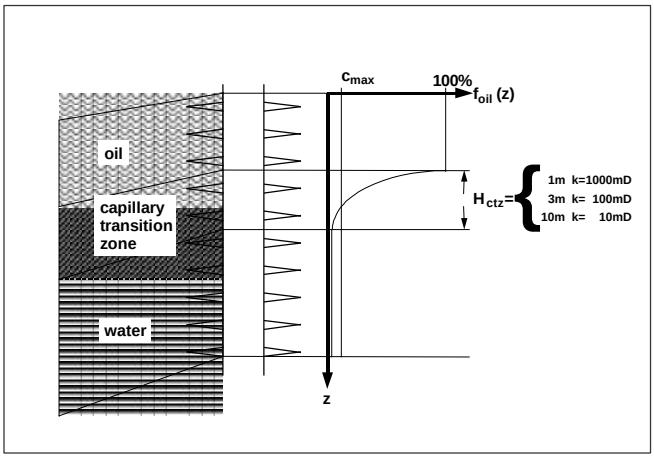

Fig.1: Vertical inflow profile of an high water-cut well

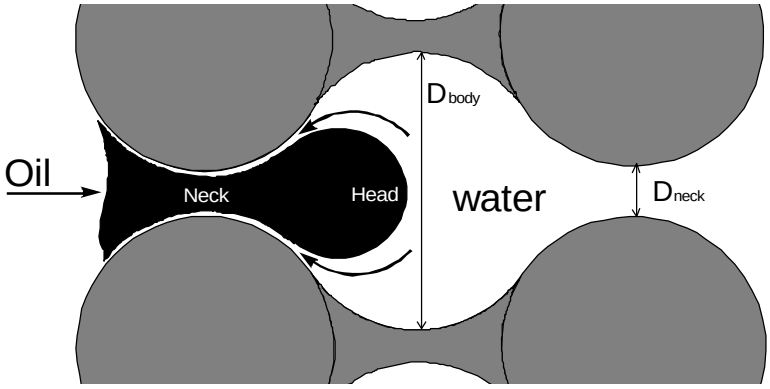

Fig.2: Snap-off process of an oil blob at a pore constriction

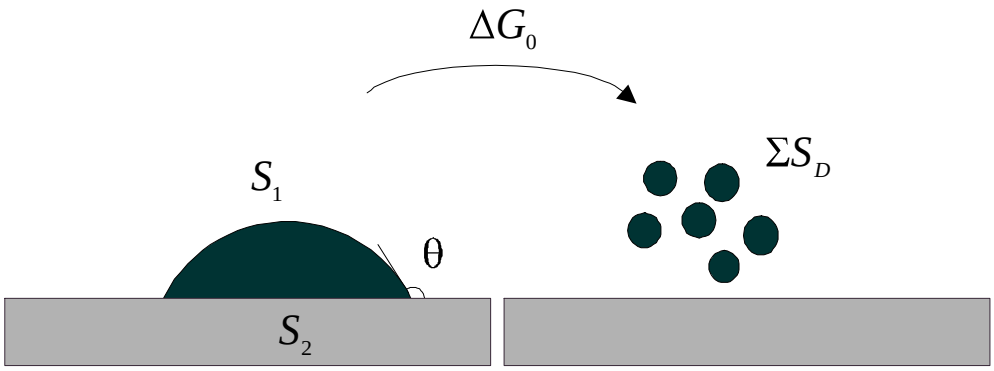

Fig.2: Detachment process of an oil drop in water from a solid substrate

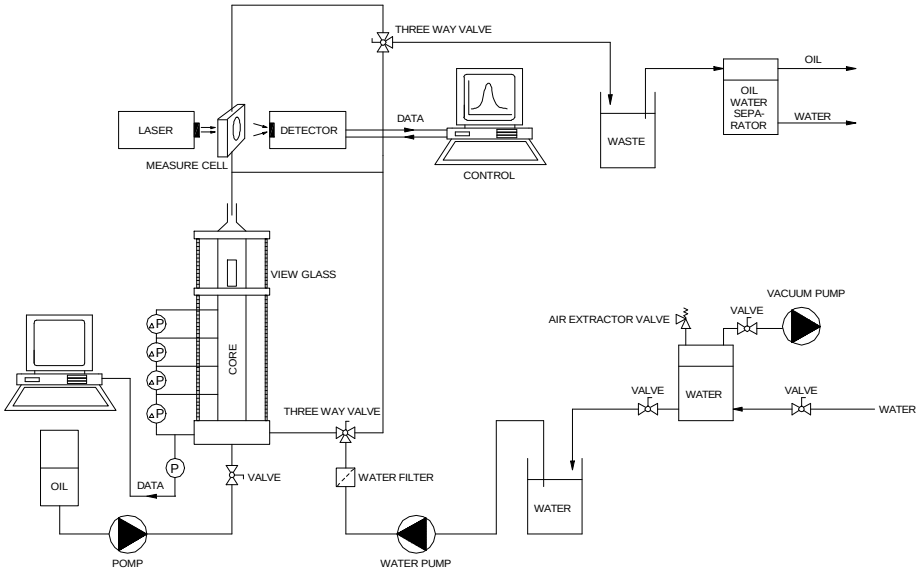

Fig.4: Set-up for core-flow experiments

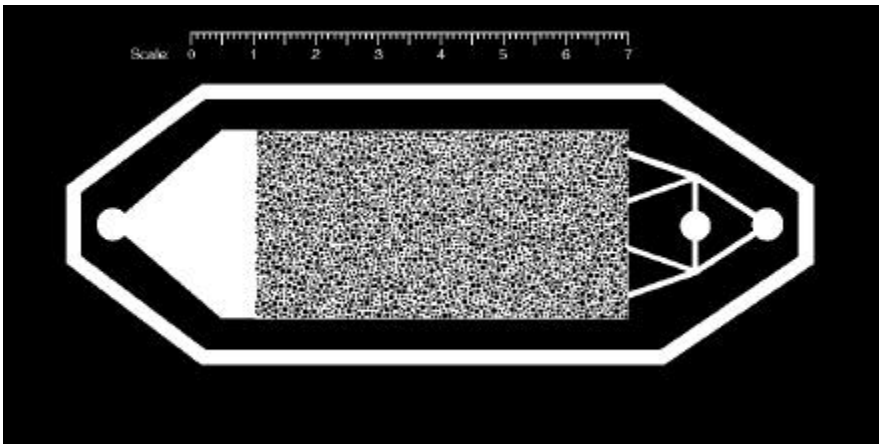

Fig.5: Micro-flow model

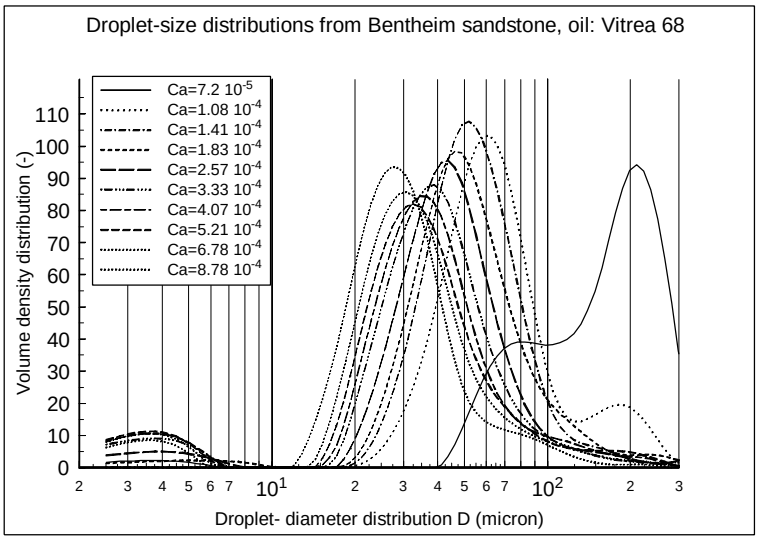

Fig.6: Typical droplet size distributions of emulsion droplets leaving water-wet sandstone for different capillary number

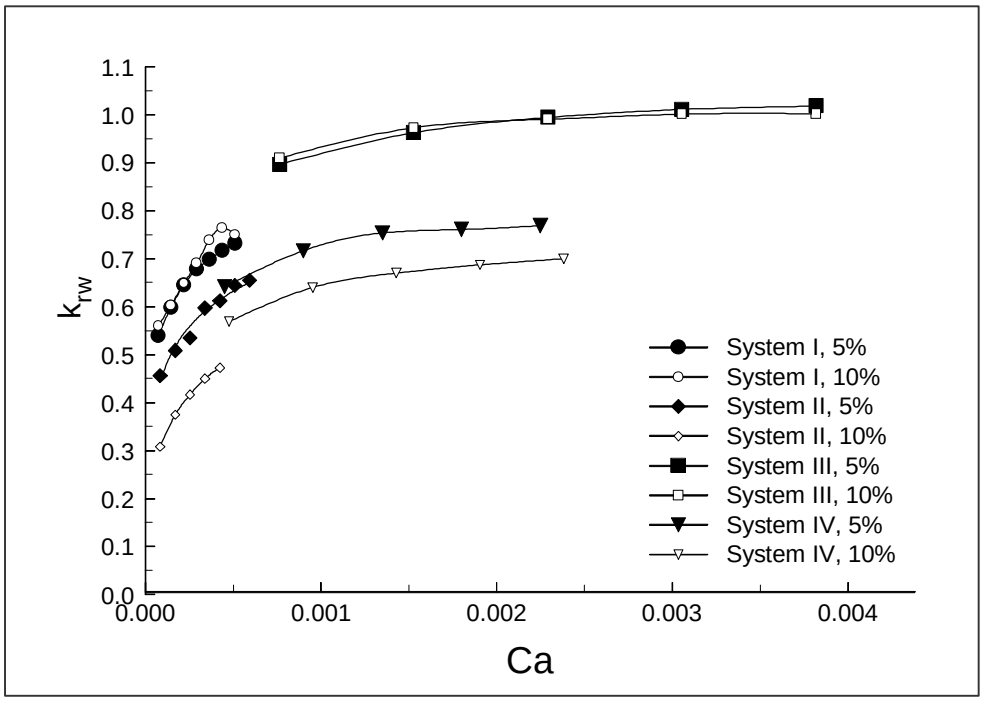

Figure 13

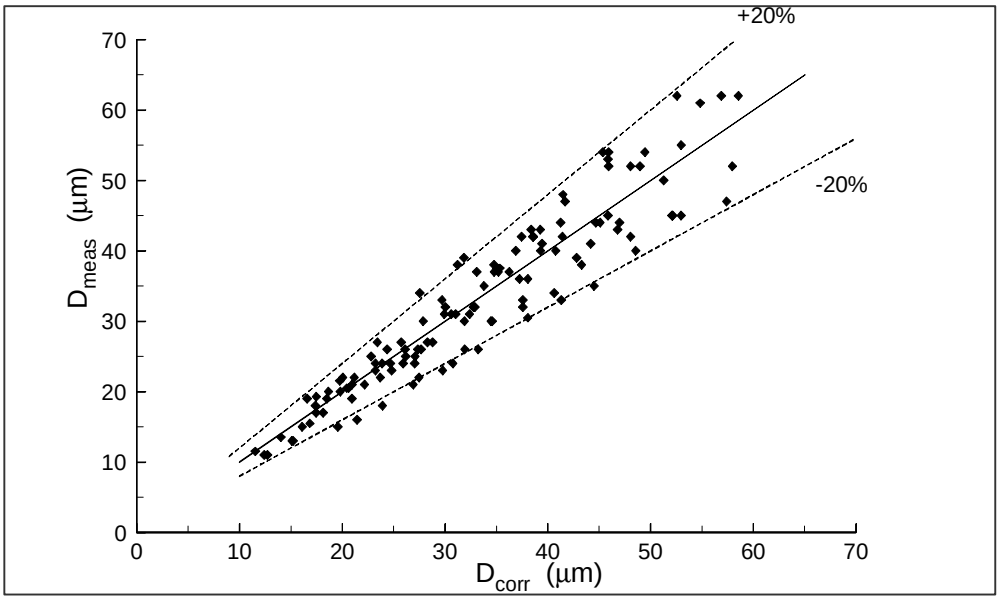

Figure 14